

Bio-mechanical Material Property Estimation Using Instrumented Laparoscopes

Abstract

Realistic simulation of tool-tissue interactions is necessary for the development of surgical simulators and one of the key element for it realism is accurate bio-mechanical tissue models. In this paper, we determined the mechanical properties of soft tissue by minimizing the difference between experimental measurements performed by instrumented laparoscopes and analytical or simulated solutions of the deformation. Using this technique, we demonstrate that one can estimate accurately the material property that best fit the experimental data compared to a simulated compression and a needle indentation with a flat-tip. We also validated our results using multiple tool-tissue interactions over the same specimen.

Keywords

Surgical simulation — Neo-Hookean — in-vivo — Bio-material — Inverse FEM — 3D Sensing — MIS

Elizabeth Mesa, System Engineering, National University of Colombia, elymesa@gmail.com

Juan Ramirez, System Engineering, National University of Colombia, juanferr@gmail.com

Pierre Boulanger, Computer Science, University of Alberta, pierreb@ualberta.ca

Introduction

Surgical simulation has revolutionized the way novice surgeons are being trained. Current training of surgeons is performed with real-life cases, instrumented phantoms, animals, cadavers, and more recently visuo-haptic simulators. Surgical simulators have been developed for a wide range of procedures and they can be classified into three main categories, needle-based, minimally invasive, and open surgery. Needle insertion is a well-known procedure due to its application in Minimally Invasive Surgeries (MIS), such as biopsies, brachytherapy, neurosurgery, and tumor ablation. Neurosurgical needle insertion is a type of MIS that is performed with a restricted field of view, displaced 2D visual feedback, and distorted haptic feedback. Much research and development have been devoted for training surgeons in MIS using visual and haptic feedback, but the accurate characterization of soft tissues for haptic simulation remains an open area of research [1].

Haptic models, which include relationships between forces and displacements during the simulated medical procedure, are usually based on biomechanical models. To simulate realistic surgical interventions for needle insertion procedures, it is necessary to implement algorithms that are accurate and are computationally efficient [2]. Furthermore, the accuracy of planning in medical interventions and the credibility of surgical simulation depend on soft-tissue constitutive laws, the shape of the surgical tool, the organ geometry, and the boundary conditions imposed by the connective tissues surrounding the organ. Because of this fidelity requirement, it is necessary to implement experimental studies to measure mechanical properties of soft tissue interaction using sensors and compare the results with tool-

tissue interaction models. Some researchers have evaluated soft tissue properties in-vivo, ex-vivo, or in phantom tissues, using stretch tests [3], aspiration experiments [4], compression tests, and needle insertion for linear [5] and non-linear bio-mechanical models [6]. In all these cases, researchers showed that their parameters correctly fit with the experimental data used in a material calibration. However, they did not evaluate the estimated material properties in different types of experimental setups by comparing the results with additional experimental data. Ultimately, one would like to be able to measure in-vivo material properties by performing simple tissue manipulations using laparoscopic tools. In order to do so we have instrumented two laparoscopes with 3D position sensors that can measure the tip location and orientation in 3D space and force/torque sensors located along the laparoscope shaft to measure the forces and torques necessary to deform the material. One can see in Figure 1 the MIS digitizing station.



Figure 1: MIS Digitizing Station

Using these measurements our goal is to develop a new tool that will be able to infer material properties of in-vivo tissues without having to perform biopsies.

For hygienic reasons and limited access to a real operation room data, we decided to perform our experiments on a silicone rubber phantom with similar mechanical properties as brain matter (see Figure 2).

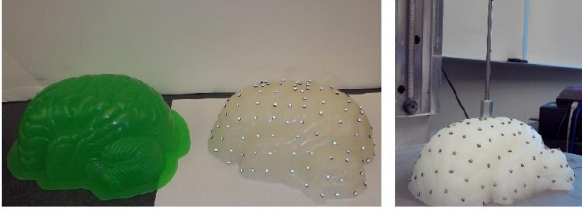


Figure 2: Ecoflex brain phantom with optical markers.

In our study, we also evaluate the effect of modeling space and material models on the accuracy of Finite Element Method (FEM) to simulate needle indentation in soft tissue. Our results can be applied to a variety of medical applications, but we focus our work on brain biopsies in which physicians use a needle. Related literature on tissue characterization and needle insertion simulation is reviewed in Section 2. In Section 3, we describe the methods and experiments to calibrate the material property and to simulate needle indentation into soft tissue. Finally in Sections 5 we discuss the experimental results. We then conclude and discuss the results obtained.

2. Related Work

Tissue characterization, also called calibration, consists of estimating material properties based on the measurement of tool-tissue interaction forces and deformations. The measurements can be done using several invasive and non-invasive techniques. Previous work on soft tissue characterization can be classified in several ways. Some researchers use indentation techniques [5][6][7], others consider stretching [3], aspiration [4], compression [8], among many others. Additionally, results have been reported on different organs from animals and humans, such as the liver [9], brain [10][11] and kidney [6]. Considering the limitations and advantages of the measurement techniques, some researchers have used ex-vivo experiments and phantom tissues, as they allow precise control of the sample and experimental conditions for modeling [5][7][12]. Finally, due to the many factors involved in soft tissue deformation, there are numerous constitutive biomechanical models that can be used to simulate different material behaviors. Some materials can be successfully defined by very simple approximations based on Hooke's Law, as shown by DiMaio and Salcudean in [5]. However, more complex materials, such as liver, kidney, and brain, require the use of viscoelastic and hyper-elastic constitutive models. Kim et al. [6] determined the hyper-viscoelastic properties of intra-abdominal organs in-vivo using an indentation device. They implemented a tridimensional inverse finite element parameter estimation algorithm and they assumed the quasi-linear-viscoelastic theory proposed by Fung [13]. As mentioned earlier, previous work on tissue calibration obtained material properties based on experimental data, but researchers usually did not evaluate and validate model performance in different applications. This is a crucial evaluation to guaranty simulator accuracy. For instance, Miller et al. [10] demonstrated that swine brain tissue is

considerably softer in extension than in compression. Therefore, these parameters should be carefully selected according to the application that needs to be simulated.

3. EXPERIMENTAL METHOD

As shown by Francheschini et al. [15], human brain tissue deforms similar to filled elastomers, and it can be modeled as a nonlinear solid with small volumetric compressibility. Girnary [16] also highlight that silicone brain phantoms provide good results to simulate brain behavior. In the present study, we determined the parameters for Neo-Hookean and Reduced Polynomial hyper-elastic models to simulate the mechanical behavior of a platinum-cure silicone rubber (Ecoflex 00-10, from Smooth-On, Inc.) submitted to a compression test. In our experiments, we used a tissue phantom rather than biological tissue because it allows us to obtain repeatable results in a controlled environment. Each component of the rubber solution was evenly mixed according to the recommendations of the manufacturer and then formed in a cylindrical mold of 38 mm diameter and 9 mm height. We used a force/torque sensor, (ATI Mini40 SI-40-2) with 0.02 N resolution, attached to a laparoscopic grasping tool, which was fixed to a rigid plate (see Figure 3).

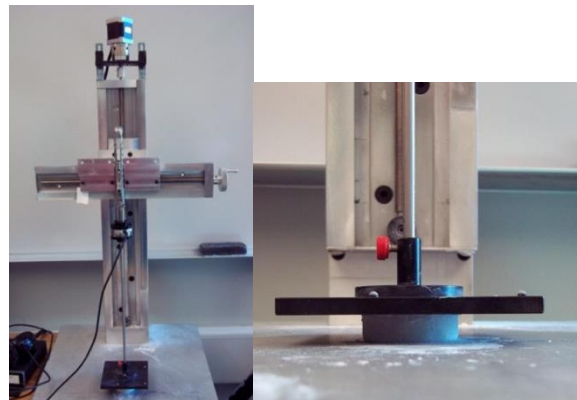


Figure 3: Experimental setup for the compression test of a silicon rubber cylinder made of Ecoflex -0010.

The surfaces were lubricated and the tissue was compressed to a strain of 0.227. The plate was displaced using a stepper motor to compress the tissue at a constant velocity of 0.4 mm/s, until the plate was displaced by 2 mm. The contact areas were lubricated with talcum powder in order to minimize lateral friction. Calibration of soft tissue consists of determining the material constants by minimizing the difference between the analytical solutions (for simple approaches) with respect to experimental measurements through a least-squares-fit procedure using the quasi-Newton method. In this study, the calibration of the material model was done using the corresponding analytical solution of the standard compression test. We used absolute errors, instead of relative errors, because this gives a better fit for large strains. The experimental nominal stress tensor was found by dividing the reaction force at every sample point by the un-deformed contact area. The nominal strain corresponded to the displacement of the plate divided by the un-deformed height of the cylinder. Once we

obtained the material parameters, we used the “evaluate” function in ABAQUS [14] to run the Drucker stability test.

We also evaluated the estimated material property by comparing different simulations of needle indentation with experimental data in order to study the influence of the material model and modeling space on the accuracy of a FEM solution. For the measurement of forces and displacement during soft tissue indentation, we used the same silicone rubber, force and torque sensors, stepper motor, and the needle was inserted at the same movement velocity. However, the specimen was a block of $70\text{ mm} \times 80\text{ mm} \times 80\text{ mm}$, and it was indented until the deformation was 10 mm (see Figure 4).

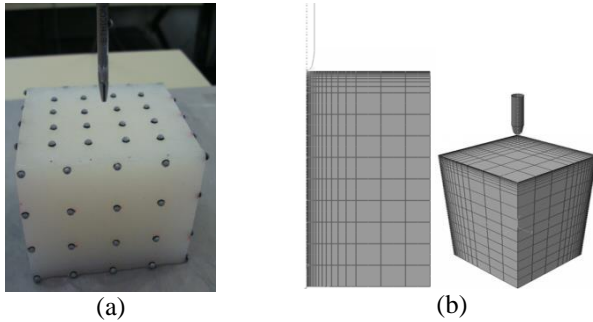


Figure 4: (a) Setup for needle indentation in a block of $70\text{ mm} \times 80\text{ mm} \times 80\text{ mm}$. We ensure that velocity is constant and the needle is indented until the strain corresponded to 0.14. (b) Mesh for the axis-symmetric (left) and 3D models (right).

The needle had a conical shape with a rounded tip of 5 mm diameter. We used a 2^k factorial design, which allowed us to find the effects of the factors and the interaction between factors [17]. The response variable was the R-Squared error between the simulation and experimental data, the factors were the material model (with levels Neo-Hookean and Reduced Polynomial) and the modeling space (with levels axis-symmetric model). Finally we performed two experiments to measure the reaction forces during the indentation, with the purpose of having a duplicate of the experiment. To run the simulation using the properties previously estimated, we simulated an indentation in ABAQUS as contact between a rigid needle and an isotropic silicone rubber. The tangential behavior of the contact was defined using a 0.8 friction coefficient. For the 3D case, we generated a cube with the same characteristics as the real specimen; for the axis-symmetric case, the model corresponded to a cylinder of 70 mm in diameter and 80 mm in height. Although this changes the approach to the problem, we will show that axis-symmetric models (which are simpler than the 3D approximation) can be used to approximate problems that are not axis-symmetric. In both cases, we used elements with hybrid formulation and reduced integration. The mesh size was graded to be more refined close to the indenter and coarser near the model boundaries (see Figure 4b). In all simulations, we allowed nonlinearities for the material model and for large geometric deformation. In the 3D approximation, the model was assumed to be symmetric, hence only one quarter of the cube needed to be simulated. The bottom of the deformable body was fixed in space, and both, the rigid indenter and the axis of symmetry (or planes of symmetry, in the 3D case) in the deformable object,

were allowed to move only in the vertical direction. We constrained the indenter tip to the node at the upper left corner of the mesh, and we moved the indenter such that the displacement amplitude changed at a rate of 0.4 mm/s until it reached 10 mm .

4. Experimental Results

The stress-strain curves for the uniaxial compression test and the predicted curves using the two hyper-elastic models are shown in Figure 5. We found $C_{10} = 1101.295$ for the Neo-Hookean material model, and $C_{10} = 686.428$; $C_{20} = 1929.606$ for the second order Reduced Polynomial Model. For the definition of those material parameters please refer to [14]. The Drucker Stability Check showed that both models were stable for all strains. The R-squared error for the fitting given by the Neo-Hookean model is 0.8965 and the error for the Reduced Polynomial model is equal to 0.9648.

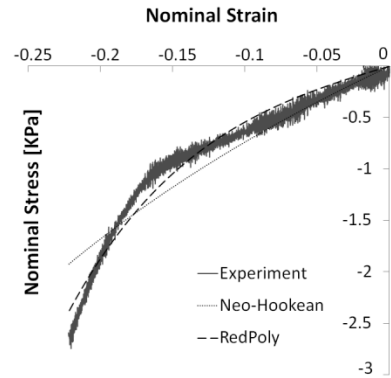


Figure 5: Material Calibration using compression test data.

Before we ran the experiments, we refined the mesh until the error of the simulation with respect to the experimental data did not change significantly. For the following experimental runs, we kept the same mesh parameters. The experimental matrix, which presents the different simulations that were run in this study and the resulting errors, is shown in Table 1. There were two runs of each simulation, and the table shows the R-Squared errors of the simulations with respect to the two experimental measurements. The results of all the FEM simulations and the experimental measurements are shown in Figure 6. In this figure we related the reaction force in the indenter with the needle displacement. The simulations differ by the parameters of the experimental design, as shown in Table 1. The simulated distributions of stresses using axis-symmetric and tridimensional models in ABAQUS are shown in Figure 7 and Figure 8.

Table 1: Experimental Matrix

Material Model (Factor A)	Modeling Space (Factor B)			
	Axisymmetric (Level 1)		3D Model (Level 2)	
Neo-Hookean (Level 1)	0.98024	0.97516	0.98931	0.98562
Reduced Polynomial (Level 2)	0.99960	0.99829	0.99976	0.99919

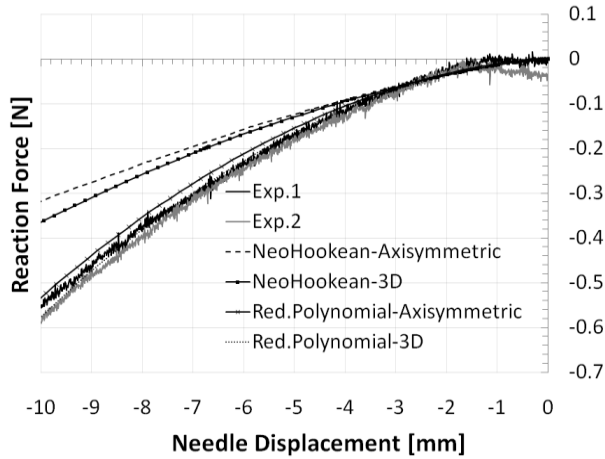


Figure 6: Comparison of experimental measurements with FEM simulations for a needle indentation.

We concluded that, for very small velocities (in our case, for "v" \approx 0.4mm/s), the material properties found in the compression test can be successfully used to simulate more complex interactions, e.g. needle indentation. We also concluded that the material model, the modeling space, and the interaction between these two factors, affect the accuracy of the simulation. However, the effect of the material model is substantially stronger than the other two. Therefore, if one needs to simulate a model that is not axis-symmetric, one can sacrifice some accuracy for a simpler and faster modeling space than the full 3D model. This is due to the fact that the effect of changing modeling space does not alter the simulation as much as changing material model. Figure 6 show that the use of a reduced polynomial material model with 3D and axis-symmetric modeling spaces gives very similar results. Bearing in mind that this silicone rubber has similar properties to brain matter, future work will focus on the characterization of phantom tissue under needle indentation (where the analytical solution is not easily defined) for possible applications of brain-tissue characterization during in-vivo experiments.

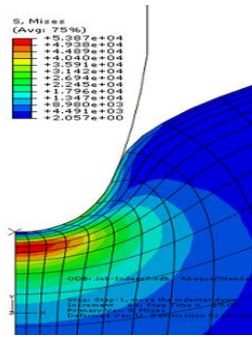


Figure 7: Axis-symmetrical Indentation in ABAQUS.

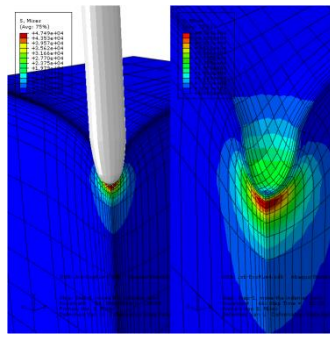


Figure 8: Mesh for the axis-symmetric (left) and 3D models (right).

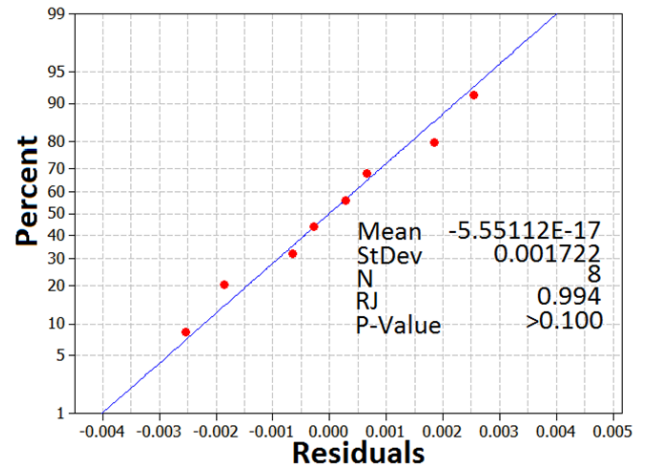


Figure 9: Normality Test – Ryan-Joiner.

An Analysis of variance (Anova) showed that the effects of the material model, the modeling space, and their interaction are statistically significant, $p = 0.001$, $p = 0.033$ and $p = 0.046$, respectively. The Anova had an acceptable adjusted error of 94.57%, where the missing 5.43% of the variability in the R-squared error of the simulation is due to the effect of factors not considered in this study. The effects sizes were $\eta^2(\text{material}) = 0.826$, $\eta^2(\text{space}) = 0.079$, and $\eta^2(\text{material} \times \text{space}) = 0.063$, indicating that the material model affect the quality of the simulation the most. We also confirmed the adequacy of the assumptions underlying the Anova [17]. The normality test using Ryan-Joiner test was not significant, $p > 0.1$, indicating that the residuals were normally distributed (see Figure 9). Furthermore, the Bartlett’s Test indicated that the residual variances were homogeneous, $p = 0.409$ (see Figure 10).

5. Conclusion

In this paper, we characterized a silicone rubber phantom using the experimental measurements from a compression test. We evaluated the effect of two material models (Neo-Hookean and a Second Order Reduced Polynomial) and two modeling spaces (axis-symmetric and 3D) on the R-squared error between simulated data and the experimental results of needle indentation.

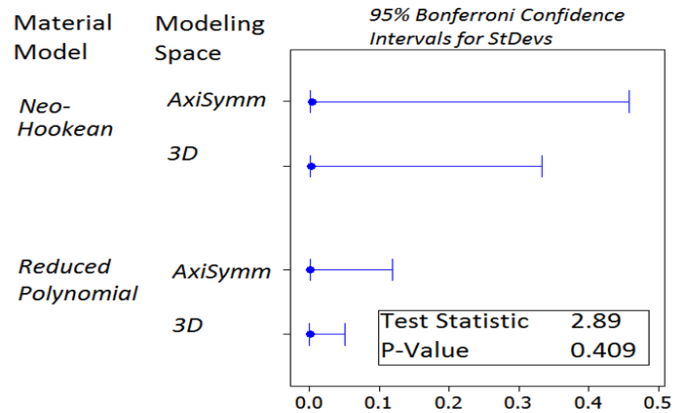


Figure 10: Bartlett’s Test for Constant Variance.

References

- [1] Abolhassani N, Patel R, Moallem M., 2007. Needle insertion into soft tissue: A survey. In: *Medical Engineering & Physics*, vol. 29, pp. 413-431.
- [2] Maciel A, Halic T, Lu Z, Nedel LP, De S., 2009. Using the PhysX engine for physics-based virtual surgery with force feedback. In: *The International Journal of Medical Robotics and Computer Assisted Surgery*, vol. 5(3), pp. 341-353.
- [3] Brouwer I, Ustin J, Bentley L, Sherman A, Dhruv N, Tendick F., 2001. Measuring in vivo animal soft tissue properties for haptic modeling in surgical simulation. In: *Studies in Health Technology and Informatics* 69-74.
- [4] Kauer M, Vuskovic V, Dual J, Szekely G, Bajka M., 2002. Inverse finite element characterization of soft tissues. In: *Medical Image Analysis*, vol. 6(3), pp. 275-287.
- [5] DiMaio SP, Salcudean S, 2003 Needle insertion modeling and simulation. In: *IEEE Transactions on Robotics and Automation*, vol. 19, pp. 864-875.
- [6] Kim J, Srinivasan MA, 2005 Characterization of viscoelastic soft tissue properties from in vivo animal experiments and inverse FE parameter estimation. In: *Medical Image Computing and Computer-Assisted Intervention-MICCAI 2005*, pp. 599-606.
- [7] Nienhuys HW, van der Stappen AF, 2004 A computational technique for interactive needle insertions in 3D nonlinear material. In: *ICRA'04. 2004 IEEE International Conference on Robotics and Automation*, vol. 2, pp. 2061-2067.
- [8] Dechwayukul C, Thongruang W., 2008. Compressive modulus of adhesive bonded rubber block. In: *Songklanakarin Journal of Science and Technology*, vol. 30(2), pp. 221-226.
- [9] Okamura AM, Simone C, O'Leary MD, 2004 Force modeling for needle insertion into soft tissue. In: *IEEE Transactions on Biomedical Engineering*, vol. 51, pp. 1707-1716.
- [10] Miller K, Wittek A, Joldes G, Horton A, Dutta-Roy T, Berger J, Morriss L., 2010. Modelling brain deformations for computer-integrated neurosurgery. In: *International Journal for Numerical Methods in Biomedical Engineering*, vol. 26(1), pp. 117-138.
- [11] Kohandel M, Sivaloganathan S, Tenti G, Drake J., 2006. The constitutive properties of the brain parenchyma: Part 1. Strain energy approach. In: *Medical engineering & physics*, vol. 28(5), pp. 449-454.
- [12] Sangpradit K, Liu H, Seneviratne LD, Althoefer K, 2009 Tissue identification using inverse Finite Element analysis of rolling indentation. In: *IEEE International Conference on Robotics and Automation ICRA'09*, pp. 1250-1255.
- [13] Fung Y, 1993. *Biomechanics: Mechanical Properties of Living Tissues*. Springer.
- [14] Simulia, Dassault Systemes. *ABAQUS Analysis User s Manual*, Version 6.9. [Internet]. 2005 [cited 2011].
- [15] Fung Y, 1965. *Foundations of Solid Mechanics*. Prentice Hall.
- [16] Franceschini G, Bigoni D, Regitnig P, Holzapfel GA., 2006. Brain tissue deforms similarly to filled elastomers and follows consolidation theory. In: *Journal of the Mechanics and Physics of Solids*, vol. 54(12), pp. 2592-2620.
- [17] Girnary HH., 2007. *Brain Phantom Project*. Master's Thesis. Cornell University.
- [18] Montgomery DC, 2001. *Design and analysis of experiments*. 5th ed. John Wiley & Sons Inc.